



**Michigan  
Technological  
University**

Michigan Technological University  
**Digital Commons @ Michigan Tech**

---

Department of Biomedical Engineering  
Publications

Department of Biomedical Engineering

---

7-23-2018

## Incorporation of anionic monomer to tune the reversible catechol-boronate complex for pH responsive, reversible adhesion

Ameya R. Narkar  
*Michigan Technological University*

Bruce P. Lee  
*Michigan Technological University*

Follow this and additional works at: <https://digitalcommons.mtu.edu/biomedical-fp>

 Part of the [Biomedical Engineering and Bioengineering Commons](#)


---

### Recommended Citation

Narkar, A. R., & Lee, B. P. (2018). Incorporation of anionic monomer to tune the reversible catechol-boronate complex for pH responsive, reversible adhesion. *Langmuir*. <http://dx.doi.org/10.1021/acs.langmuir.8b00373>

Retrieved from: <https://digitalcommons.mtu.edu/biomedical-fp/34>

Follow this and additional works at: <https://digitalcommons.mtu.edu/biomedical-fp>

 Part of the [Biomedical Engineering and Bioengineering Commons](#)

1 Incorporation of Anionic Monomer to Tune the  
2 Reversible Catechol-Boronate Complex for pH  
3 Responsive, Reversible Adhesion

4

5 *Ameya R. Narkar and Bruce P. Lee\**

6 Department of Biomedical Engineering, Michigan Technological University, Houghton, MI  
7 49931.

8 KEYWORDS: Smart adhesive, acrylic acid, catechol-boronate complexation, reversible  
9 adhesion.

10

11 ABSTRACT

12 Up to 30 mol% of acrylic acid (AAc) was incorporated into a pH responsive smart adhesive  
13 consisting of dopamine methacrylamide (DMA) and 3-acrylamido phenylboronic acid (APBA).  
14 FTIR spectroscopy and rheometry confirmed that the incorporation of AAc shifted the pH of  
15 catechol-boronate complexation to a more basic pH. Correspondingly, adhesive formulations with  
16 elevated AAc contents demonstrated strong adhesion to quartz substrate at a neutral to mildly basic  
17 pH (pH 7.5-8.5) based on Johnson-Kendall-Roberts (JKR) contact mechanics test. When pH was  
18 further increased to pH 9.0, there was a drastic reduction in the measured work of adhesion (18

1 and 7 fold reduction compared to values measured at pH 7.5 and 8.5, respectively) due to the  
2 formation of catechol-boronate complex. The complex remained reversible and the interfacial  
3 binding property of the adhesive was successfully tuned with changing pH in successive contact  
4 cycles. However, an acidic pH (pH 3.0) was required to break the catechol-boronate complex to  
5 recover the elevated adhesive property. Adding AAC enables the smart adhesive to function in  
6 physiological or marine pH ranges.

7

## 8 INTRODUCTION

9 Smart adhesives can transform reversibly between its adhesive and non-adhesive states with an  
10 externally applied stimulus. This property is particularly important for the development of painless  
11 and removal dressings, sustainable packaging materials, recyclable bonded structures, and robust  
12 walking mechanisms for microrobotics.<sup>1-4</sup> Currently available smart adhesives are limited by the  
13 need for elevated temperatures for debonding,<sup>3</sup> adhesion to a specific substrate,<sup>5</sup> or poor adhesion  
14 in a wet environment.<sup>4</sup> In particular, the presence of a liquid layer on the substrate acts as an  
15 obstacle to adhesion, making most synthetic adhesives ineffective in a wet environment.<sup>6-8</sup>

16 Mussels secrete adhesive proteins that contain a catecholic amino acid, 3,4-  
17 dihydroxyphenylalanine (DOPA), which enables them to bind to wet substrates.<sup>6,9</sup> In its reduced  
18 form, catechol has the ability to interact inorganic surfaces (e.g., metals) through formation of  
19 coordination bonds, while in its oxidized form, it is capable of forming interfacial covalent bonds  
20 with organic surfaces (e.g., tissues).<sup>10,11</sup> Incorporating catechol into inert polymers has imparted  
21 these materials with strong, wet adhesive properties for various applications.<sup>12-14</sup> Several labs have

1 recently reported different catechol-based adhesives that are responsive to light,<sup>15</sup> enzyme,<sup>16</sup> or  
2 temperature.<sup>17</sup>

3 The adhesive property of catechol is highly dependent on its oxidation state.<sup>18-21</sup> At an acidic pH,  
4 catechol is in its reduced state, and forms strong interfacial bonds with inorganic substrates.<sup>10</sup>  
5 However, when the pH approaches the dissociation constant of catechol ( $pK_a \approx 9.3$ ), catechol is  
6 progressively oxidized and its strength of interfacial interaction is significantly reduced.<sup>10</sup>  
7 Recently, we exploited this pH-dependent adhesive property of catechol to design a smart  
8 adhesive.<sup>22</sup> This adhesive consisted of both network-bound catechol and boronic acid, which  
9 demonstrated elevated adhesion at pH 3.0. At pH 9.0, the formation of catechol-boronate complex  
10 reduced the measured work of adhesion by over an order of magnitude. Boronic acid not only  
11 contributed to adhesion, but also protected catechol from irreversible oxidation and crosslinking.  
12 Even though the ideal pH for catechol-boronate complexation is 9.0,<sup>22, 23</sup> the complex forms  
13 readily at a neutral and mildly basic pH,<sup>24</sup> which will limit the potential for using this smart  
14 adhesive for applications at physiological or marine pH ranges (i.e., pH 7.5-8.5).<sup>25, 26</sup>

15 To tune the pH of catechol-boronate complexation, we introduced an acidic anionic monomer,  
16 acrylic acid (AAc), into the adhesive network. Incorporating an acidic moiety has been  
17 demonstrated to preserve the catechol in its reduced state.<sup>27, 28</sup> Similarly, we previously  
18 demonstrated that the incorporation of AAc preserved the reduced and adhesive state of catechol  
19 even at a pH of 8.5, potentially due to the localized buffering capacity of the carboxylic acid side  
20 chain.<sup>29</sup> We hypothesized that incorporating AAc will shift the catechol-boronate complexation  
21 pH to a more basic pH, and thus control the pH at which the adhesive transitions between adhesive  
22 and non-adhesive states.

1 To this end, we synthesized adhesives containing dopamine methacrylamide (DMA), 3-  
2 acrylamido phenylboronic acid (APBA) and AAc consisting of an adhesive catechol moiety,  
3 protective boronic acid functional group, and an anionic –COOH side chain, respectively.  
4 Johnson–Kendall–Roberts (JKR) contact mechanics tests were carried out to determine the effect  
5 of AAc concentration on adhesion over a wide range of pH (3.0-9.0). Additionally, Fourier-  
6 transform infrared (FTIR) spectroscopy and rheometry experiments were used to characterize the  
7 effect of AAc on the formation of the catechol-boronate complex.

8

9

## 10 MATERIALS AND METHODS

### 11 Materials

12 APBA, AAc, *N*-hydroxyethyl acrylamide (HEAA), trichloro(1*H*,1*H*,2*H*,2*H*-perfluorooctyl)silane  
13 (97%), and toluene (anhydrous, 99.8%) were purchased from Sigma-Aldrich (St. Louis, MO).  
14 Methylene bis-acrylamide (MBAA) and 2,2-dimethoxy-2-phenylacetophenone (DMPA) were  
15 purchased from Acros Organics (New Jersey, USA). Dimethyl sulfoxide (DMSO) was purchased  
16 from Macron (Center Valley, PA), and ethanol (200 proof) was purchased from Pharmco Aaper  
17 (Brookfield, CT). DMA was synthesized by following previously published protocols.<sup>30</sup> Quartz  
18 slides were purchased from Ted Pella (Redding, CA). The acidic pH 3.0 solution was prepared by  
19 adding appropriate quantities of 1 M HCl to a solution containing 0.1 M NaCl, while pH 7.5, 8.5,  
20 and 9.0 buffers were prepared by adjusting the pH of 10 mM Tris (hydroxymethyl)aminomethane  
21 (Tris) buffer containing 0.1 M NaCl with 1 M HCl.<sup>29</sup> Fluorinated glass slides were prepared by

1 submerging glass slides (Fisher Scientific; cat. no. 12-550-A3; Hampton, NH) in a solution  
2 containing 0.5 mL of trichloro(1*H*,1*H*,2*H*,2*H*-perfluorooctyl)silane and 49 mL of toluene for 20  
3 min, washed three times with fresh toluene, and air-dried.<sup>22</sup>

#### 4 Preparation of the Adhesive

5 Adhesive hydrogels were prepared by curing precursor solutions containing 1 M HEAA with 10  
6 mol % of DMA, 10 mol % of APBA and 0–30 mol % of AAc dissolved in 40 % (v/v) DMSO and  
7 deionized (DI) water. The cross-linker (MBAA) and photoinitiator (DMPA) were kept constant at  
8 3 and 0.1 mol %, respectively. All of the monomer, cross-linker, and photoinitiator concentrations  
9 in the precursor solutions were reported in relation to the concentration of the HEAA (**Scheme**  
10 **S1**). Precursor solutions were degassed three times with N<sub>2</sub> gas and added to a mold composed of  
11 two pieces of glass separated by a silicone rubber spacer (2.0 mm thick). All samples were  
12 photocured in an ultraviolet (UV) cross-linking chamber (XL-1000, Spectronics Corporation;  
13 Westbury, NY) placed inside a N<sub>2</sub>-filled glovebox (Plas Laboratories; Lansing, MI) for a total of  
14 600 s.<sup>29, 31, 32</sup> After the curing process, all samples were washed in a pH 3.0 solution overnight to  
15 remove any unreacted monomers. Samples for swelling and rheometry experiments were formed  
16 into a disk shape using a punch with a diameter of 7.9 mm. They were further rinsed twice in  
17 deionized (DI) water and equilibrated at the desired pH for 24 h with constant nutation. For contact  
18 mechanics tests, hemispherical samples were prepared by irradiating 50  $\mu$ L of the precursor  
19 solution on a hydrophobic, fluorinated glass slide with UV and purified in the similar manner as  
20 described above.<sup>29</sup> Adhesive compositions were abbreviated as DxByAz where x, y and z denote  
21 the mol % of DMA, APBA and AAc respectively, in relation to HEAA.

22

1     Equilibrium Swelling

2     Hydrogel discs (thickness = 2.0 mm and diameter = 7.9 mm) were equilibrated at different pH  
3     levels for 24 h, and then dried in vacuum for at least 48 h. The masses of the swollen ( $M_s$ ) and  
4     dried ( $M_d$ ) samples were obtained to determine the equilibrium swelling ratio by using the  
5     equation:<sup>29</sup>

$$\text{Equilibrium Swelling} = \frac{M_s}{M_d} \quad (1)$$

6     FTIR

7     The samples were freeze-dried, crushed into powder using a mortar and pestle, and analyzed using  
8     a PerkinElmer Frontier Spectrometer fitted with a GladiATR<sup>TM</sup> accessory from Pike Technologies.

9     Oscillatory Rheometry

10    Hydrogel discs (thickness = 2.0 mm and diameter = 7.9 mm), were compressed to a fixed gap of  
11    1800  $\mu\text{m}$  using an 8 mm diameter parallel plate geometry. The storage ( $G'$ ) and loss ( $G''$ ) moduli  
12    were determined in the frequency range of 0.1-100 Hz and at a constant strain of 8 % using a TA  
13    Discovery Hybrid Rheometer-2 (TA Instruments; New Castle, DE).

14    Contact Mechanics Test

15    JKR contact mechanics tests were performed using a custom-built setup comprising of a 10-g load  
16    cell (Transducer Techniques; Temecula, CA) and a miniature linear stage stepper motor (MFA-  
17    PPD, Newport; Irvine, CA). Hemispherical adhesives were affixed to an indenter stem (ALS-06,  
18    Transducer Techniques; Temecula, CA) using Super Glue (Adhesive Systems MG 100) and  
19    compressed at a rate of 1  $\mu\text{m}/\text{sec}$  against a buffer-wetted quartz surface until a fixed maximum

1 preload of 20 mN was reached (**Figure S1**).<sup>22, 29</sup> The hemispheres were then retracted at the same  
2 speed. One contact cycle comprised of bringing the hemispheres into contact with the substrate at  
3 a constant speed until the fixed preload was reached and then retracting it at the same speed.

4 Two types of adhesion tests were performed. For the first test, samples were equilibrated at pH  
5 3.0, 7.5, 8.5 or 9.0 for 24 h and tested against a quartz slide wetted with 25  $\mu$ L of buffer with the  
6 same pH to determine the effect of AAc concentration on interfacial binding properties at these  
7 different pH levels. For the second test, adhesives were examined for their ability to switch  
8 between adhesive and non-adhesive states in response to pH. A single sample was subjected to 3  
9 successive contact cycles. Samples were first incubated at pH 7.5 for 3 h. The first and the second  
10 contacts were carried out in the presence of pH 7.5 and 9.0, respectively, while the third contact  
11 was carried out in the presence of either pH 7.5, or pH 3.0. Between two cycles, the samples were  
12 incubated for 30 min in a custom-built well that contained  $\approx$  350  $\mu$ L of either pH 9.0 (between first  
13 and second cycle), or pH 7.5 or 3.0 (between second and third cycles) buffer solution. In order to  
14 ensure that the target pH was reached before testing (i.e., pH 9.0 for incubation prior to the second  
15 cycle), the custom-built well was rinsed twice with  $\approx$  350  $\mu$ L of buffer with the desired pH before  
16 the start of the subsequent cycle. Additionally, the medium used to incubate the hemispherical  
17 adhesive was changed every 10 min during the 30 min incubation period.

18 The force (F) versus displacement ( $\delta$ ) curves were integrated to determine the work of adhesion  
19 ( $W_{adh}$ ), which was normalized by the maximum area of contact ( $A_{max}$ ) by using the following  
20 equation:<sup>22</sup>

$$21 \quad W_{adh} = \frac{\int F d\delta}{A_{max}} \quad (2)$$

22



1  $A_{\max}$  was calculated by fitting the loading portion of the F versus  $\delta$  curve with the Hertzian  
2 model.<sup>33</sup>

$$3 \quad \delta_{\max} = \frac{a^2}{R}, \quad (3)$$

4 where  $\delta_{\max}$  is the maximum displacement at the maximum preload of 20 mN, a is the radius  
5 of  $A_{\max}$ , and R is the curvature of the hemispherical sample. The height (h) and base radius (r) of  
6 each hemisphere were measured using digital Vernier calipers before the start of each test to  
7 determine R.<sup>34</sup>

$$8 \quad R = \frac{h}{2} + \frac{r^2}{2h} \quad (4)$$

9  $A_{\max}$  was calculated by using the equation:

$$10 \quad A_{\max} = \pi a^2 \quad (5)$$

11 The adhesion strength ( $S_{\text{adh}}$ ) was calculated by normalizing the maximum pull-off force ( $F_{\max}$ ) by  
12 the maximum area of contact ( $A_{\max}$ ) using the equation:<sup>35</sup>

$$13 \quad S_{\text{adh}} = \frac{F_{\max}}{A_{\max}} \quad (6)$$

#### 14 Statistical Analysis

15 Statistical analysis was performed using JMP Pro 13 application (SAS Institute, NC). One-way  
16 analysis of variance (ANOVA) with Tukey-Kramer HSD analysis was performed for comparing  
17 means.  $p < 0.05$  was considered significant.

18

19

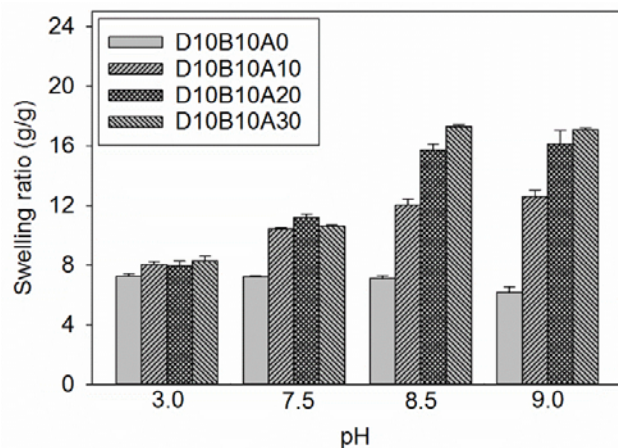
1

## 2 RESULTS AND DISCUSSION

3 Up to 30 mol % of AAc was formulated into an adhesive hydrogel containing DMA and APBA  
4 and its effect on the formation of catechol-boronate complex and interfacial binding property were  
5 evaluated over a wide range of pH (3.0-9.0). pH 3.0 was chosen because the adhesive properties  
6 of catechol with inorganic substrates at this pH have been widely documented.<sup>20, 29</sup> Additionally,  
7 we have previously confirmed that adhesives containing both DMA and APBA do not form  
8 complex at this pH.<sup>22</sup> pH 7.5 and 8.5 were chosen to represent physiological and marine pH  
9 ranges.<sup>25, 26</sup> pH 9.0 was selected to promote the formation of the catechol-boronate complex and  
10 to inactivate the adhesive.<sup>22</sup>

### 11 Equilibrium Swelling

12 Equilibrium swelling tests were performed to confirm the addition of AAc in the adhesives. The  
13 equilibrium swelling ratio of AAc-containing adhesives increased with increasing pH (**Figure 1**).  
14 Additionally, formulations containing higher AAc concentrations also demonstrated higher  
15 increase in swelling with increasing pH. For example, the equilibrium swelling ratio of  
16 D10B10A30 exhibited the highest difference between values measured at pH 9.0 and 3.0 (over 2  
17 fold increase). The carboxylic acid side chain of AAc becomes progressively deprotonated with  
18 increasing pH ( $pK_a \approx 4.25$ ).<sup>36</sup> The negatively charged AAc resulted in charge repulsion of the  
19 polymer chains and increased the swelling ratio of the adhesive network.<sup>37</sup>

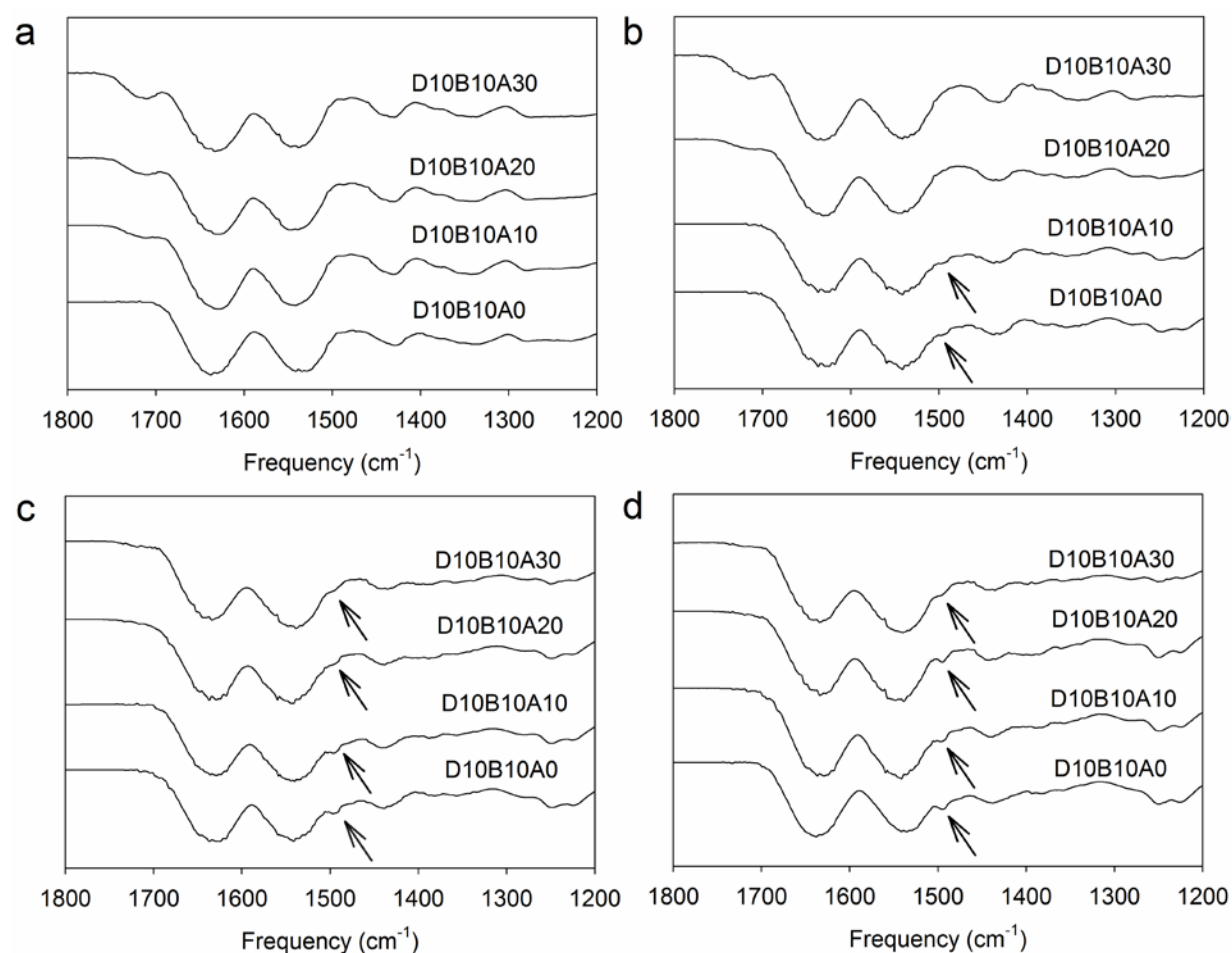


1  
2 **Figure 1.** Equilibrium swelling ratio for adhesive equilibrated at pH 3.0, 7.5, 8.5 or 9.0 for 24 h  
3 (n = 3). Refer to **Table S1** for statistical analysis.

4  
5 **FTIR**

6 All adhesive formulations exhibited signature peaks for HEAA ( $-\text{OH}$   $3400\text{-}3000\text{ cm}^{-1}$ , secondary  
7 amide  $-\text{NH}$   $1680\text{-}1630\text{ cm}^{-1}$ , and  $\text{C}=\text{O}$   $1600\text{-}1500\text{ cm}^{-1}$ ), and benzene rings ( $1500\text{-}1400$  and  $800\text{-}$   
8  $700\text{ cm}^{-1}$ ) in their FTIR spectra (**Figures 2 and S2**).<sup>31,38</sup> Formulations containing AAc also exhibit  
9 characteristic peak of carboxylic acid ( $-\text{C}=\text{O} \approx 1700\text{ cm}^{-1}$ ),<sup>38</sup> which increased in peak intensity  
10 with increasing AAc content in the adhesive (**Figure 2a**). With increasing pH, formulations  
11 containing both DMA and APBA exhibited a new peak at  $1490\text{ cm}^{-1}$  (arrows in **Figure 2**). This  
12 peak corresponds to the benzene ring stretch as a result of catechol-boronate complexation.<sup>22, 39</sup>  
13 For formulations with no AAc or low AAc content (e.g., D10B10A0 and D10B10A10,  
14 respectively), this new peak appeared at a pH as low as 7.5 (**Figure 2b**). For formulations with  
15 higher AAc concentrations (e.g., D10B10A20 and D10B10A30), the complexation peak was not  
16 observed until a pH of 8.5 (**Figure 2c**). FTIR results confirmed that the presence of the acidic AAc  
17 monomer interfered with the formation of catechol-boronate complexation, potentially due to the

1 ability of the network-bound anion to maintain a more acidic pH environment within the adhesive  
2 network. Adhesive formulations with elevated AAc contents required a higher pH in the incubation  
3 medium to form the complex. FTIR spectra for formulations that did not contain both DMA and  
4 APBA (e.g., D0B10A20, D10B0A20) did not exhibit a peak at  $1490\text{ cm}^{-1}$  (**Figure S2**), further  
5 confirming that this peak is attributed to the catechol-boronate complex.



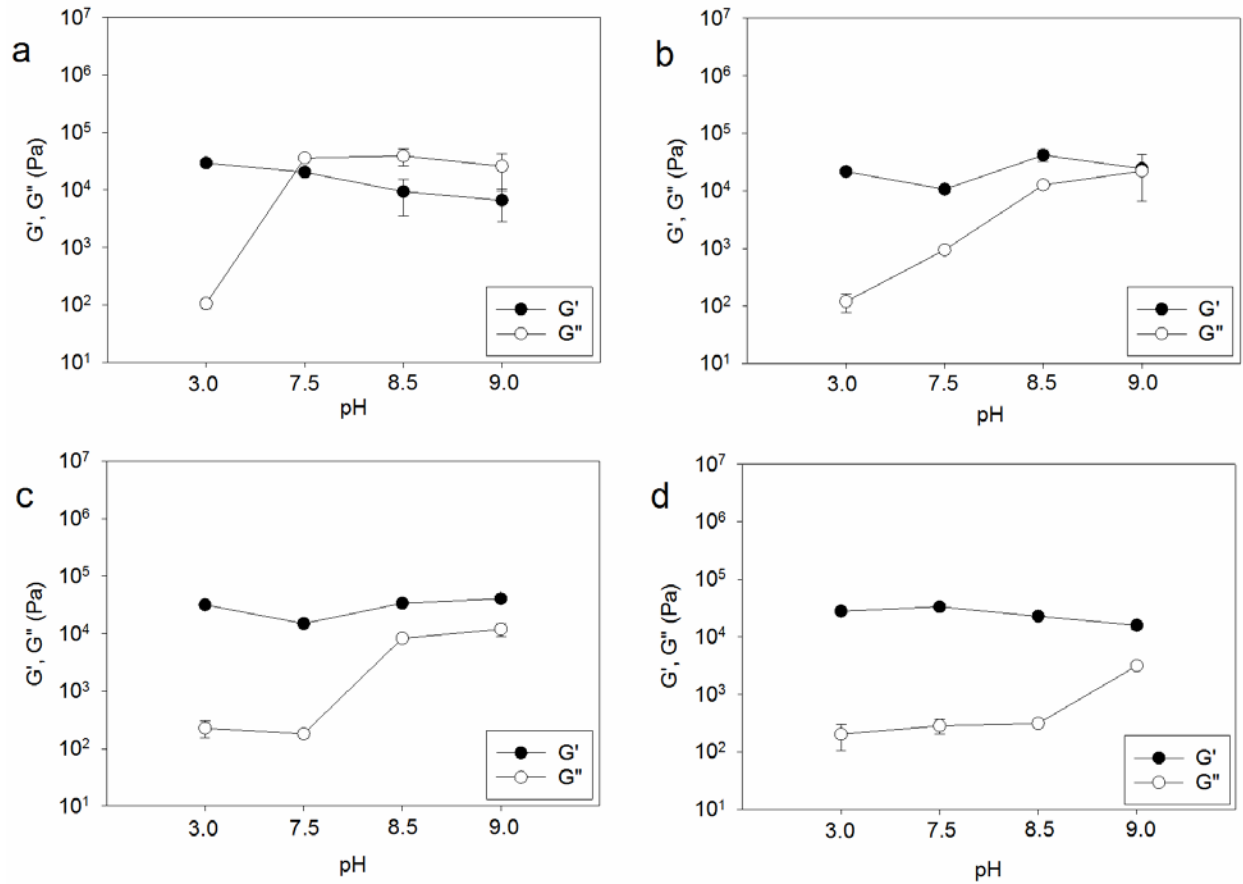
6  
7 **Figure 2.** FTIR spectra of adhesive equilibrated at pH 3.0 (a), pH 7.5 (b), pH 8.5 (c) or pH 9.0  
8 (d). The arrows indicate peaks corresponding to formation of the catechol-boronate complex at  
9  $1490\text{ cm}^{-1}$ .

10  
11

## 1 Oscillatory Rheometry

2 Frequency sweep experiments were performed to determine the storage and loss moduli ( $G'$  and  
3  $G''$ , respectively) of the adhesive (**Figure S3**) and the values obtained at a frequency of 1 Hz were  
4 further summarized in **Figure 3**. For all the adhesive formulations,  $G'$  values were comparable  
5 (averaged around  $10^4$  Pa) and did not change greatly with changing pH. Contrastingly,  $G''$  values  
6 increased by 1 to 2 orders of magnitude with increasing pH. An elevated  $G''$  value corresponded  
7 to the dissipation of reversible physical bonds between catechol and boronic acid within the  
8 polymer network.<sup>40,41</sup> We have previously observed a similar pH-induced change in the measured  
9  $G''$  values as a result of catechol-boronate complexation.<sup>22</sup> For D10B10A0, the onset of change in  
10 the  $G''$  values occurred between pH 3.0 and 7.5 (**Figure 3a**). With increasing AAc content, a higher  
11 solution pH was required to induce a similar increase in the  $G''$  values. For D10B10A30,  $G''$  values  
12 remained constant around  $10^2$  Pa and did not increase to  $10^3$  Pa until pH 9.0. Rheometry data  
13 corroborated FTIR data in showing that the presence of AAc interfered with the catechol-boronate  
14 complexation. Specifically, the pH responsive nature of the complex correlated with the  
15 concentration of the anionic monomer. Formulations that did not contain both DMA and APBA  
16 (e.g., D0B10A20 and D10B0A20) did not exhibit a large increase in the measured  $G''$  values with  
17 increasing pH (**Figure S4**).

18



1  
 2 **Figure 3.** Storage ( $G'$ , filled symbols) and loss ( $G''$ , empty symbols) moduli for D10B10A0 (a),  
 3 D10B10A10 (b), D10B10A20 (c) and D10B10A30 (d) equilibrated at pHs 3.0, 7.5, 8.5 or 9.0  
 4 tested at a frequency of 1 Hz and 8 % strain ( $n = 3$ ).

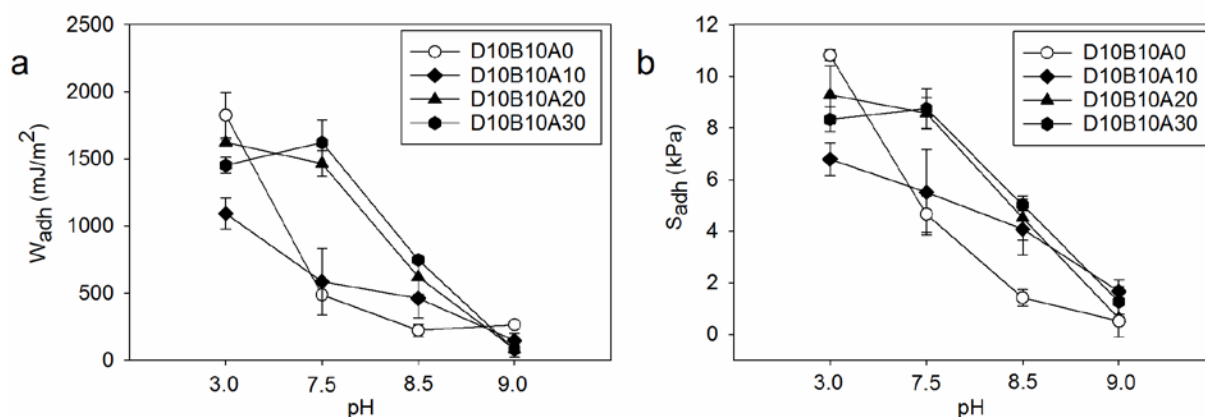
5 Contact Mechanics Test: Single Contact

6 JKR contact mechanics test was performed to determine the effect of AAc concentration on  
 7 interfacial binding property over a wide range of pH (3.0-9.0) using quartz ( $\text{SiO}_2$ ) surface as the  
 8 test substrate (**Figure 4**). Adhesive formulation without AAc (e.g., D10B10A0) exhibited the  
 9 strongest adhesive interaction with quartz at pH 3.0 ( $W_{\text{adh}} = 1830 \pm 170 \text{ mJ/m}^2$ ,  $S_{\text{adh}} = 10.8 \pm 0.209$   
 10 kPa), when both the reduced form of catechol and the boronic acid contributed to strong interfacial  
 11 interaction (i.e., hydrogen bonding) with the quartz surface.<sup>10, 22</sup> Correspondingly, all formulations

1 exhibited low  $G''$  values ( $\approx 10^2$  Pa, **Figure 3**). When D10B10A0 was incubated at a pH of 7.5 or  
2 higher, there was a significant decrease in the measured adhesive values ( $W_{\text{adh}} = 487 \pm 21.9$  mJ/m<sup>2</sup>,  
3  $S_{\text{adh}} = 4.66 \pm 0.704$  kPa for pH 7.5). The measured adhesive values for D10B10A0 further  
4 decreased with increasing pH ( $W_{\text{adh}} = 264 \pm 10.1$  mJ/m<sup>2</sup>,  $S_{\text{adh}} = 0.515 \pm 0.613$  kPa for pH 9.0).  
5 Both FTIR and rheometry results (**Figures 2 and 3**, respectively) indicated that catechol-boronate  
6 complexation formed at a pH as low as 7.5 for D10B10A0, suggesting that the formation of the  
7 complex limited the availability of the adhesive molecules for interfacial binding. A large  
8 reduction in the measured adhesive values at a neutral to mildly basic pH made D10B10A0  
9 impractical for many applications at this pH range. Additionally, at low AAc concentration, the  
10 adhesive values for D10B10A10 at pH 3.0 were lower than the other tested formulations. This is  
11 perhaps due to the H-bond interactions between AAc chains in the bulk,<sup>42</sup> which interfered with  
12 the ability of catechol to form interfacial bonds.

13 Incorporating 20 mol % or higher AAc resulted in a significant increase in the measured adhesive  
14 values at both pH 7.5 and 8.5 (**Figure 4 and Table S2**). For example, measured  $W_{\text{adh}}$  values for  
15 D10B10A20 and D10B10A30 equilibrated at pH 7.5 were 3 fold higher when compared to those  
16 measured for D10B10A0. This indicated that network-bound AAc was able to counteract the  
17 solution pH and maintain a local acidic pH within the adhesive network.<sup>29</sup> At pH 7.5, no catechol-  
18 boronate complex peaks were observed for both D10B10A20 and D10B10A30 (**Figure 2b**), and  
19 these formulations also exhibited low  $G''$  values ( $\approx 10^2$  Pa; **Figures 3c and 3d**). These observations  
20 further suggest that both DMA and APBA were available for strong interfacial binding at pH 7.5.  
21 With further increase in pH, measured adhesive values decreased. At pH 8.5, both D10B10A20  
22 and D10B10A30 showed complexation peak in their FTIR spectra (**Figure 2c**), which  
23 correspondingly resulted in reduced adhesion, and D10B10A20 also exhibited high  $G''$  values ( $\approx$

1  $10^4$  Pa), while  $G''$  values of D10B10A30 continued to remain low ( $\approx 10^2$  Pa). However, values  
 2 measured at pH 8.5 were still around 3 fold higher when compared to those measured for  
 3 D10B10A0. Regardless of adhesive formulation, lowest adhesive values were measured at pH 9.0,  
 4 and all formulations exhibited high  $G''$  values ( $10^3 - 10^4$  Pa, **Figure 3**). Although the incorporation  
 5 of AAc preserved the interfacial binding property of the adhesive at a neutral to mild basic pH, the  
 6 anion lost its buffering capability at an elevated pH, which was corroborated with elevated  $G''$   
 7 values. Nevertheless, the  $W_{adh}$  values for D10B10A20 at pH 7.5 and pH 8.5 were 18 and 7 fold  
 8 higher, respectively, when compared to values measured at pH 9.0. This difference in the measured  
 9 adhesive values makes the adhesive a good candidate to function as a smart adhesive.



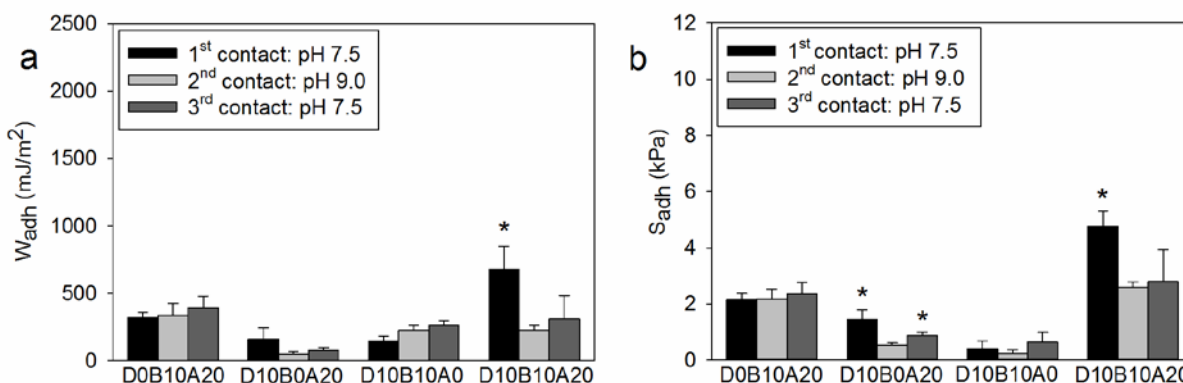
10  
 11 **Figure 4.** Work of adhesion ( $W_{adh}$ ) (a) and adhesion strength ( $S_{adh}$ ) (b) for single contact  
 12 experiments tested between wetted quartz substrate and adhesive equilibrated at pH 3.0, 7.5, 8.5  
 13 or 9.0 ( $n = 3$ ). Refer to **Table S2** for statistical analysis.

14 **Contact Mechanics Test: Reversible Adhesion Testing**

15 To evaluate the feasibility for AAc to control the pH responsive characteristics of the catechol-  
 16 boronate complex, adhesive samples were subjected to three successive contact cycles at pH 7.5,  
 17 9.0 and then at 7.5 again (**Figure 5**). D10B10A20 showed strong adhesion during the first contact



1 at pH 7.5 ( $W_{adh} = 677 \pm 173 \text{ mJ/m}^2$ ,  $S_{adh} = 4.76 \pm 0.557 \text{ kPa}$ ) and significantly reduced adhesion  
 2 during the second contact at pH 9.0 ( $W_{adh} = 230. \pm 33.2 \text{ mJ/m}^2$ ,  $S_{adh} = 2.59 \pm 0.185 \text{ kPa}$ ) as  
 3 expected. However, the adhesion values remained low for the final contact at pH 7.5 ( $W_{adh} = 311$   
 4  $\pm 174 \text{ mJ/m}^2$ ,  $S_{adh} = 2.80 \pm 1.13 \text{ kPa}$ ). The adhesive samples were incubated for only 30 min at pH  
 5 7.5 in between the last two contact cycles and may not have had sufficient ionic exchange to break  
 6 the strong, reversible complex. D10B10A0 was not responsive to changes in pH as the catechol-  
 7 boronate complexation readily formed at a pH 7.5 and higher and it does not contain anionic  
 8 monomer to modulate complexation pH.



9  
 10 **Figure 5.** Averaged  $W_{adh}$  (a) and  $S_{adh}$  (b) for adhesives tested in three successive contact cycles  
 11 using quartz as the substrate ( $n = 3$ ). \*  $p < 0.05$  relative to the values obtained from the second  
 12 contact cycle at pH 9.0 for a given formulation.

13 To confirm the reversible nature of the catechol-boronate complex, the pH for the third contact  
 14 cycle was lowered to 3.0 (**Figures 6** and **S5**). D10B10A20 exhibited elevated and reduced  
 15 adhesion at pH 7.5 ( $W_{adh} = 663 \pm 65.1 \text{ mJ/m}^2$ ,  $S_{adh} = 5.63 \pm 0.488 \text{ kPa}$ ) and 9.0 ( $W_{adh} = 85.9 \pm$   
 16  $47.6 \text{ mJ/m}^2$ ,  $S_{adh} = 1.34 \pm 1.03 \text{ kPa}$ ), respectively, as observed in the previous series of reversible  
 17 adhesion testing (**Figure 5**). However, when the pH was decreased to 3.0 during the third contact  
 18 cycle, the adhesive recovered its adhesive properties ( $W_{adh} = 1540 \pm 171 \text{ mJ/m}^2$ ,  $S_{adh} = 6.99 \pm$

1 0.983 kPa). The measured  $W_{adh}$  and  $S_{adh}$  values were 17 and 5 fold higher, respectively, when  
2 compared to values measured for the second contact at pH 9.0. Similarly, D10B10A0 exhibited  
3 low adhesive properties during the first two contact cycles conducted at pH 7.5 and 9.0, but  
4 recovered elevated adhesive properties during the third contact cycle conducted at pH 3.0 ( $W_{adh} =$   
5  $1800 \pm 439 \text{ mJ/m}^2$ ,  $S_{adh} = 9.20 \pm 1.19 \text{ kPa}$ ). These observations indicate that the catechol-boronate  
6 complex within the adhesive remained reversibly bonded, and an acidic pH was required to break  
7 the complex and recover the strong interfacial binding.

8 During both series of reversible adhesion testing (**Figures 5 and 6**), the presence of boronic acid  
9 in D0B10A20 contributed to adhesion potentially via hydrogen bonding or electrostatic  
10 interaction.<sup>22</sup> However, D0B10A20 did not demonstrate pH responsive adhesive property,  
11 indicating that the presence of boronic acid alone was not sufficient to design a smart adhesive.  
12 D10B0A20 demonstrated reversible adhesion resulting from pH dependent oxidation and  
13 reduction of the catechol moiety. Although catechol readily oxidizes at a pH of 7.5, the presence  
14 of the network-bound anion preserved the reduced state of catechol for strong adhesion.<sup>29</sup> AAc  
15 lost its buffering capacity when the pH was increased to pH 9.0. However, pH 7.5 was insufficient  
16 to reduce catechol for strong adhesion and pH 3.0 was required to recover its adhesive property.  
17 This observation further confirmed that poor ion diffusion is the main factor that limited pH  
18 responsive property of the hydrogel based adhesive. Although D10B0A20 was pH responsive, the  
19 measured adhesion values were relatively low when compared to D10B10A20. This confirms our  
20 previous findings that both catechol and boronic acid contributed to strong adhesion.<sup>22</sup>

1  
2  
3  
4  
5  
6  
7  
8  
9  
10  
11  
12  
13  
14  
15  
16  
17

**Figure 6.** Averaged  $W_{adh}$  (a) and  $S_{adh}$  (b) for adhesives tested in three successive contact cycles using quartz as the substrate ( $n = 3$ ). \*  $p < 0.05$  relative to the values obtained from the second contact cycle at pH 9.0 for a given formulation.

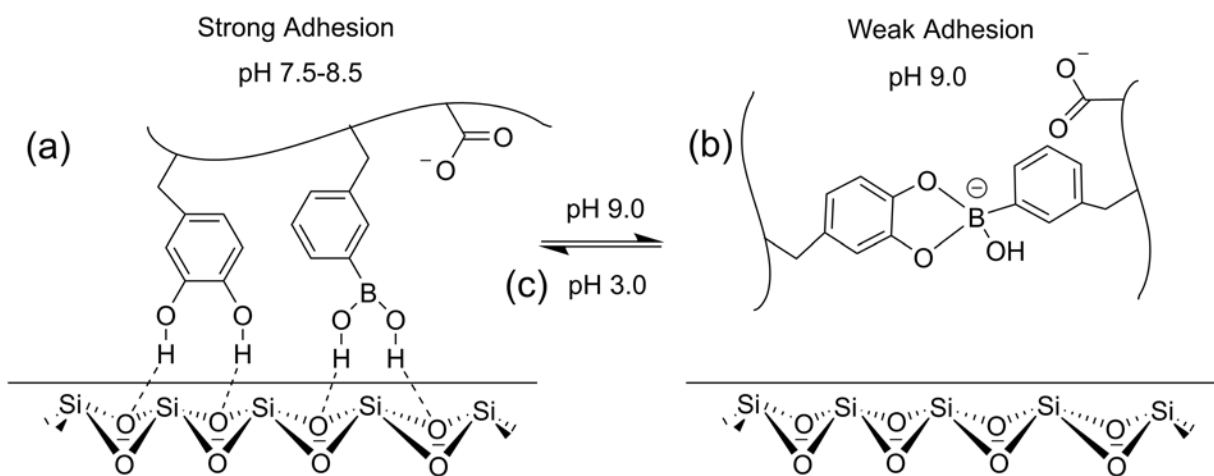
The ideal pH for complexation between catechol ( $pK_a = 9.3$ )<sup>43</sup> and phenylboronic acid ( $pK_a = 8.8$ )<sup>43, 44</sup> has been reported to be the average of their respective pKa values ( $(9.3+8.8)/2 \approx 9$ ).<sup>24</sup> As such, the complex forms as the pH approached 9 and resulted in poor adhesion at a neutral and mildly basic pH. The addition of AAc acidified the local pH within the adhesive network and shifted the pH for catechol-boronate complexation to a more basic pH. This disruption of the complex permitted both catechol and phenylboronic acid to participate in strong interfacial binding at pH 7.5 to 8.5 (**Scheme 1**). Incorporation of elevated amount of AAc did not prevent complexation at pH 9.0, which is necessary for the inactivation of the adhesive. Although the JKR technique used to calculate  $W_{adh}$  takes into account only the maximum area of contact and minimizes the sample volume to reduce losses due to the bulk dissipation within the adhesive hydrogel, the hysteresis in the JKR curves which indicates a likely contribution of bulk dissipative behavior due to pH responsive changes in the adhesive network, would require further probing.<sup>45-</sup>

<sup>47</sup> The incorporation of AAc provides an effective strategy for designing adhesives for applications

1 that demand strong adhesion at physiological or marine pH levels, while preserving the adhesive's  
2 ability to transition between its adhesive and non-adhesive states in response to pH.

3  
4

5 **Scheme 1.** Schematic representation of a smart adhesive consisting of acrylic acid in addition to  
6 catechol and phenylboronic acid interacting with a wetted quartz substrate.



7

8 The presence of the anionic AAc reduced local pH, which prevented catechol-boronate  
9 complexation while enabled these adhesive molecules to form strong interfacial bonds with the  
10 quartz substrate even at a neutral mildly basic pH (a). When the pH was raised to a more basic  
11 value (i.e. pH 9.0), AAc lost its buffering capacity, which resulted in the formation of the catechol-  
12 boronate complex while inactivating the adhesive (b). Decreasing the solution pH to pH 3.0,  
13 effectively breaks the catechol-boronate complex and recovers strong interfacial binding behavior  
14 of the adhesive molecules (c).

15

## 16 CONCLUSIONS

17 DMA and APBA-containing adhesive hydrogels were formulated with up to 30 mol % of AAc to  
18 tune the pH responsive characteristics of catechol-boronate complexation. FTIR and rheometry  
19 confirmed that formulations with elevated AAc contents required a higher pH to form the catechol-  
20 boronate complex, which corresponded to elevated adhesive property measured at a neutral to

1 mildly basic pH (pH 7.5-8.5). This is potentially due to the ability for the anionic AAc side chain  
2 to acidify the local pH within the adhesive network. At pH 9.0, measured adhesive values reduced  
3 dramatically due to the formation of the catechol-boronate complex. The catechol-boronate  
4 complex remained reversible and the interfacial binding property of the adhesive was successfully  
5 tuned with changing pH in successive contact cycles. However, an acidic pH (pH 3.0) was required  
6 to break the catechol-boronate complex to recover the elevated adhesive property.

7

## 8 ASSOCIATED CONTENT

### 9 **Supporting information**

10 Schematic showing the chemical structures, statistical analysis for equilibrium swelling data,  
11 photograph of the contact mechanics setup, FTIR data, additional rheometry data, contact curves  
12 for adhesives and statistical analysis for  $W_{adh}$  and  $S_{adh}$  of adhesives tested against a wetted quartz  
13 substrate.

14

## 15 AUTHOR INFORMATION

16 Corresponding Author

17 \*Bruce P. Lee. E-mail: [bplee@mtu.edu](mailto:bplee@mtu.edu)

18 Funding Sources

19 This project was supported by the Office of Naval Research Young Investigator Award under  
20 Award Number N00014-16-1-2463.

1 Notes

2 The authors declare no competing financial interest.

3

4 ACKNOWLEDGEMENT

5 We thank Randall Wilharm for the synthesis of DMA.

6

7 REFERENCES

- 8 1. Heinzmann, C.; Coulibaly, S.; Roulin, A.; Fiore, G. L.; Weder, C., Light-Induced  
9 Bonding and Debonding with Supramolecular Adhesives. *ACS Appl. Mater. Interfaces* **2014**, *6*,  
10 (7), 4713-4719.
- 11 2. Banea, M. D.; da Silva, L. F. M.; Carbas, R. J. C.; de Barros, S., Debonding on command  
12 of multi-material adhesive joints. *The Journal of Adhesion* **2017**, *93*, (10), 756-770.
- 13 3. Luo, X.; Lauber, K. E.; Mather, P. T., A thermally responsive, rigid, and reversible  
14 adhesive. *Polymer* **2010**, *51*, (5), 1169-1175.
- 15 4. Northen, M. T.; Greiner, C.; Arzt, E.; Turner, K. L., A Gecko-Inspired Reversible  
16 Adhesive. *Adv. Mater.* **2008**, *20*, (20), 3905-3909.
- 17 5. Sudre, G.; Olanier, L.; Tran, Y.; Hourdet, D.; Creton, C., Reversible adhesion between a  
18 hydrogel and a polymer brush. *Soft Matter* **2012**, *8*, (31), 8184-8193.
- 19 6. Lee, B. P.; Messersmith, P. B.; Israelachvili, J. N.; Waite, J. H., Mussel-inspired  
20 adhesives and coatings. *Annu. Rev. Mater. Res.* **2011**, *41*, 99-132.

- 1 7. Waite, J. H., Nature's underwater adhesive specialist. *Int. J. Adhes. Adhes.* **1987**, 7, (1), 9-  
2 14.
- 3 8. Comyn, J., *The relationship between joint durability and water diffusion*. Applied  
4 Science Publishers: London, 1981.
- 5 9. Lu, Q.; Danner, E.; Waite, J. H.; Israelachvili, J. N.; Zeng, H.; Hwang, D. S., Adhesion of  
6 mussel foot proteins to different substrate surfaces. In *J. R. Soc., Interface*, 2013; Vol. 10, p  
7 20120759.
- 8 10. Lee, H.; Scherer, N. F.; Messersmith, P. B., Single-molecule mechanics of mussel  
9 adhesion. *Proc. Natl. Acad. Sci. U. S. A.* **2006**, 103, (35), 12999-13003.
- 10 11. Waite, J. H., The phylogeny and chemical diversity of quinone-tanned glues and  
11 varnishes. *Comparative Biochemistry and Physiology Part B: Comparative Biochemistry* **1990**,  
12 97, (1), 19-29.
- 13 12. Meredith, H. J.; Wilker, J. J., The interplay of modulus, strength, and ductility in  
14 adhesive design using biomimetic polymer chemistry. *Adv. Funct. Mater.* **2015**, 25, (31), 5057-  
15 5065.
- 16 13. Pechey, A.; Elwood, C. N.; Wignall, G. R.; Dalsin, J. L.; Lee, B. P.; Vanjcek, M.;  
17 Welch, I.; Ko, R.; Razvi, H.; Cadieux, P. A., Anti-adhesive coating and clearance of device  
18 associated uropathogenic *Escherichia coli* cystitis. *The Journal of urology* **2009**, 182, (4), 1628-  
19 1636.
- 20 14. Liu, Y.; Meng, H.; Konst, S.; Sarmiento, R.; Rajachar, R.; Lee, B. P., Injectable  
21 dopamine-modified poly (ethylene glycol) nanocomposite hydrogel with enhanced adhesive  
22 property and bioactivity. *ACS Appl. Mater. Interfaces* **2014**, 6, (19), 16982-16992.

- 1 15. Shafiq, Z.; Cui, J.; Pastor-Pérez, L.; San Miguel, V.; Gropeanu, R. A.; Serrano, C.; del  
2 Campo, A., Bioinspired Underwater Bonding and Debonding on Demand. *Angew. Chem. Int. Ed.*  
3 **2012**, 51, (18), 4332-4335.
- 4 16. Wilke, P.; Helfricht, N.; Mark, A.; Papastavrou, G.; Faivre, D.; Börner, H. G., A Direct  
5 Biocombinatorial Strategy toward Next Generation, Mussel-Glue Inspired Saltwater Adhesives.  
6 *J. Am. Chem. Soc.* **2014**, 136, (36), 12667-12674.
- 7 17. Zhao, Y.; Wu, Y.; Wang, L.; Zhang, M.; Chen, X.; Liu, M.; Fan, J.; Liu, J.; Zhou, F.;  
8 Wang, Z., Bio-inspired reversible underwater adhesive. *Nat. Commun.* **2017**, 8, (1), 2218.
- 9 18. Deming, T. J., Synthetic polypeptides for biomedical applications. *Prog. Polym. Sci.*  
10 **2007**, 32, (8), 858-875.
- 11 19. Lee, B. P.; Chao, C.-Y.; Nunalee, F. N.; Motan, E.; Shull, K. R.; Messersmith, P. B.,  
12 Rapid Gel Formation and Adhesion in Photocurable and Biodegradable Block Copolymers with  
13 High DOPA Content. *Macromolecules* **2006**, 39, (5), 1740-1748.
- 14 20. Yu, J.; Wei, W.; Menyo, M. S.; Masic, A.; Waite, J. H.; Israelachvili, J. N., Adhesion of  
15 Mussel Foot Protein-3 to TiO<sub>2</sub> Surfaces: the Effect of pH. *Biomacromolecules* **2013**, 14, (4),  
16 1072-1077.
- 17 21. Guvendiren, M.; Messersmith, P. B.; Shull, K. R., Self-Assembly and Adhesion of  
18 DOPA-Modified Methacrylic Triblock Hydrogels. *Biomacromolecules* **2008**, 9, (1), 122-128.
- 19 22. Narkar, A. R.; Barker, B.; Clisch, M.; Jiang, J.; Lee, B. P., pH Responsive and Oxidation  
20 Resistant Wet Adhesive based on Reversible Catechol–Boronate Complexation. *Chem. Mater.*  
21 **2016**, 28, (15), 5432-5439.



- 1 23. He, L.; Fullenkamp, D. E.; Rivera, J. G.; Messersmith, P. B., pH responsive self-healing  
2 hydrogels formed by boronate–catechol complexation. *Chem. Commun.* **2011**, 47, (26), 7497-  
3 7499.
- 4 24. Yan, J.; Springsteen, G.; Deeter, S.; Wang, B., The relationship among pKa, pH, and  
5 binding constants in the interactions between boronic acids and diols—it is not as simple as it  
6 appears. *Tetrahedron* **2004**, 60, (49), 11205-11209.
- 7 25. Waugh, A.; Grant, A., *Ross & Wilson Anatomy and Physiology in Health and Illness E-*  
8 *Book*. Elsevier Health Sciences: 2010.
- 9 26. Chester, R.; Jickells, T., *Marine Geochemistry*. Wiley-Blackwell Publishing: 2012.
- 10 27. Moulay, S.; Mehdaoui, R., Hydroquinone/catechol-bearing polyacrylic acid: redox  
11 polymer. *React. Funct. Polym.* **2004**, 61, (2), 265-275.
- 12 28. Wang, W.; Xu, Y.; Li, A.; Li, T.; Liu, M.; von Klitzing, R.; Ober, C. K.; Kayitmazer, A.  
13 B.; Li, L.; Guo, X., Zinc induced polyelectrolyte coacervate bioadhesive and its transition to a  
14 self-healing hydrogel. *Rsc Advances* **2015**, 5, (82), 66871-66878.
- 15 29. Narkar, A. R.; Kelley, J. D.; Pinnaratip, R.; Lee, B. P., Effect of Ionic Functional Groups  
16 on the Oxidation State and Interfacial Binding Property of Catechol-Based Adhesive.  
17 *Biomacromolecules* **2017**.
- 18 30. Lee, H.; Lee, B. P.; Messersmith, P. B., A reversible wet/dry adhesive inspired by  
19 mussels and geckos. *Nature* **2007**, 448, (7151), 338-341.
- 20 31. Lin, M.-H.; Narkar, A.; Konst, S.; Wilharm, R., Modulating the movement of hydrogel  
21 actuator based on catechol–iron ion coordination chemistry. *Sens. Actuators, B* **2015**, 206, 456-  
22 462.

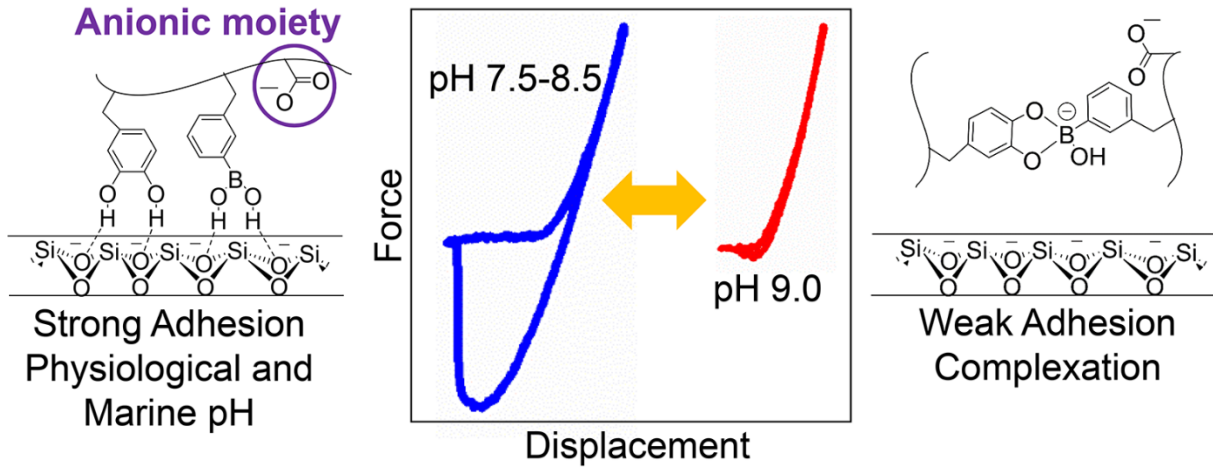
- 1 32. Lee, B. P.; Konst, S., Novel hydrogel actuator inspired by reversible mussel adhesive  
2 protein chemistry. *Adv. Mater.* **2014**, 26, (21), 3415-3419.
- 3 33. Hertz, H., On the contact of elastic solids. *J. Reine Angew Math.* **1881**, 92, 156-171.
- 4 34. Shull, K. R.; Chen, W.-L., Fracture mechanics studies of adhesion in biological systems.  
5 *Interface Sci.* **2000**, 8, (1), 95-110.
- 6 35. Burkett, J. R.; Wojtas, J. L.; Cloud, J. L.; Wilker, J. J., A Method for Measuring the  
7 Adhesion Strength of Marine Mussels. *The Journal of Adhesion* **2009**, 85, (9), 601-615.
- 8 36. Jin, X.; Hsieh, Y.-L., pH-responsive swelling behavior of poly (vinyl alcohol)/poly  
9 (acrylic acid) bi-component fibrous hydrogel membranes. *Polymer* **2005**, 46, (14), 5149-5160.
- 10 37. Nesrinne, S.; Djamel, A., Synthesis, characterization and rheological behavior of pH  
11 sensitive poly (acrylamide-co-acrylic acid) hydrogels. *Arabian J. Chem.* **2017**, 10, (4), 539-547.
- 12 38. Kirwan, L. J.; Fawell, P. D.; van Bronswijk, W., In Situ FTIR-ATR Examination of  
13 Poly(acrylic acid) Adsorbed onto Hematite at Low pH. *Langmuir* **2003**, 19, (14), 5802-5807.
- 14 39. Chen, G. C., Synthesis and evaluation of aminoborates derived from boric acid and diols  
15 for protecting wood against fungal and thermal degradation. *Wood Fiber Sci.* **2008**, 40, (2), 248-  
16 257.
- 17 40. Li, Y.; Meng, H.; Liu, Y.; Narkar, A.; Lee, B. P., Gelatin Microgel Incorporated  
18 Poly(ethylene glycol)-Based Bioadhesive with Enhanced Adhesive Property and Bioactivity.  
19 *ACS Appl. Mater. Interfaces* **2016**, 8, (19), 11980-11989.
- 20 41. Holten-Andersen, N.; Harrington, M. J.; Birkedal, H.; Lee, B. P.; Messersmith, P. B.;  
21 Lee, K. Y. C.; Waite, J. H., pH-induced metal-ligand cross-links inspired by mussel yield self-  
22 healing polymer networks with near-covalent elastic moduli. *Proc. Natl. Acad. Sci. U. S. A.*  
23 **2011**, 108, 2651-2655.

- 1 42. Zhao, J.; Burke, N. A.; Stöver, H. D., Preparation and study of multi-responsive  
2 polyampholyte copolymers of N-(3-aminopropyl) methacrylamide hydrochloride and acrylic  
3 acid. *RSC Adv.* **2016**, 6, (47), 41522-41531.
- 4 43. Springsteen, G.; Wang, B., A detailed examination of boronic acid–diol complexation.  
5 *Tetrahedron* **2002**, 58, (26), 5291-5300.
- 6 44. Bull, S. D.; Davidson, M. G.; van den Elsen, J. M. H.; Fossey, J. S.; Jenkins, A. T. A.;  
7 Jiang, Y.-B.; Kubo, Y.; Marken, F.; Sakurai, K.; Zhao, J.; James, T. D., Exploiting the  
8 Reversible Covalent Bonding of Boronic Acids: Recognition, Sensing, and Assembly. *Acc.*  
9 *Chem. Res.* **2013**, 46, (2), 312-326.
- 10 45. Crosby, A. J.; Shull, K. R., Adhesive failure analysis of pressure-sensitive adhesives. *J.*  
11 *Polym. Sci., Part B: Polym. Phys.* **1999**, 37, (24), 3455-3472.
- 12 46. Vaenkatesan, V.; Li, Z.; Vellinga, W.-P.; de Jeu, W. H., Adhesion and friction behaviours  
13 of polydimethylsiloxane—A fresh perspective on JKR measurements. *Polymer* **2006**, 47, (25),  
14 8317-8325.
- 15 47. Torres, J. R.; Jay, G. D.; Kim, K. S.; Bothun, G. D., Adhesion in hydrogel contacts.  
16 *Proceedings. Mathematical, Physical, and Engineering Sciences / The Royal Society* **2016**, 472,  
17 (2189), 20150892.

18

19

1 TOC



2